Int. J. Multiphase Flow Vol. 16, No. 1, pp. 79–89, 1990
Printed in Great Britain.

0301-9322/90 $3.00 + 0.00

EFFECT OF BUBBLE SHAPE ON PRESSURE DROP CALCULATIONS IN VERTICAL SLUG FLOW

D. BARNEA

Department of Fluid Mechanics and Heat Transfer, Faculty of Engineering, Tel-Aviv University, Ramat-Aviv 69978, Israel

(*Received* 28 *October* 1988; *in revised form* 6 *June* 1989)

Abstract—Hydrodynamic models for vertical slug flow usually consider a cylindrical Taylor bubble with a flat nose. Based on these models, two different methods have been used in the past for the calculation of the pressure drop. The first one incorporates an acceleration term, whereas this term is missing in the second one. In this work it is shown that the difference between the two methods results from the neglect of the nose shape. When the curved shape of the nose is considered the two methods yield identical results. Some approximate methods that do not consider the nose shape are tested and compared to the case where the nose shape is accounted for.

Key Words: slug flow, pressure drop

INTRODUCTION

Any method for calculating the pressure drop in slug flow is based on the *a priori* knowledge of the hydrodynamic parameters of the slug. The pressure drop is not determined unless the bubble length, the liquid slug length, the translational velocity, the liquid holdup and velocity of the liquid film, are specified separately.

Hydrodynamic models for vertical slug flow were presented with various degrees of accuracy by Taitel *et al.* (1980), Taitel & Barnea (1983), Fernandes *et al.* (1983) (who proposed a detailed hydrodynamic model), Orell & Rembrand (1986) and Sylvester (1987). However, all the above models considered a cylindrical Taylor bubble with a uniform film thickness along the bubble. This simplification, although allowing a relatively simple solution, may lead to an inconsistent calculation of the pressure drop and affects the pressure drop results considerably.

MOTIVATION

Figure 1 shows schematically the geometry of a stable slug flow, where the Taylor bubble is assumed to be cylindrical with a flat nose. Since usually the gas density and viscosity are much lower than the liquid density and viscosity, the gas in the Taylor bubble is substantially at a constant pressure, the interfacial shear is negligible and the liquid film is assumed to flow downwards around the Taylor bubble as a free falling film. A frequently used method for pressure drop calculation is to divide the pressure drop along a slug unit into two parts (Fernandes *et al.* 1983; Taitel & Barnea 1983; Sylvester 1987): the pressure drop along the body of the bubble, which is zero; and the pressure drop in the liquid slug which consists of

(a) the pressure drop due to acceleration across the mixing zone in the front of the liquid slug—ΔP_{acc},
(b) the pressure loss due to frictional effects in the liquid slug—ΔP_{fs} and
(c) the pressure drop due to the hydrostatic head of the liquid slug—ΔP_{gs}.

Thus, the total pressure loss across one slug unit becomes:

$$\Delta P_t = \Delta P_{acc} + \Delta P_{fs} + \Delta P_{gs}. \quad [1]$$

An alternative and equivalent method for pressure drop calculation is to use a global force balance between planes A–A and B–B (figure 1). The momentum fluxes in and out are identical

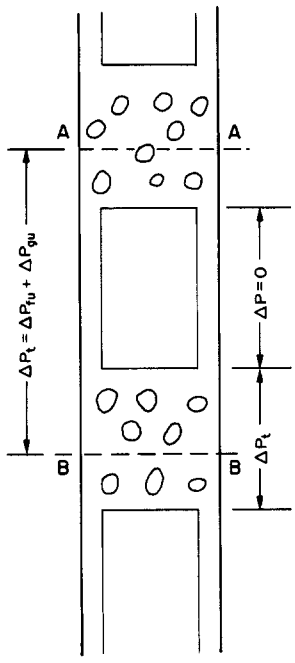

Figure 1. Slug flow with cylindrical Taylor bubbles.

and the pressure drop across this control volume consists of the frictional pressure drop ΔP_{fu} and the hydrostatic pressure drop ΔP_{gu} along the slug unit, namely:

$$\Delta P_t = \Delta P_{fu} + \Delta P_{gu}, \quad [2]$$

where ΔP_{fu} is composed of the frictional losses along the liquid slug, ΔP_{fs}, and the frictional pressure drop along the falling film, ΔP_{ff}. The gravitational losses along the slug unit ΔP_{gu} are composed of ΔP_{gs} and the hydrostatic head of the liquid film ΔP_{gf}. Thus, the total pressure drop is

$$\Delta P_t = \Delta P_{fs} + \Delta P_{gs} + \Delta P_{ff} + \Delta P_{gf}. \quad [3]$$

Since the liquid film flowing around the Taylor bubble is considered to be a free falling film with a negligible interfacial shear and of a constant film thickness, ΔP_{ff} is balanced by ΔP_{gf} which leads to the following total pressure drop between planes A–A and B–B:

$$\Delta P_t = \Delta P_{fs} + \Delta P_{gs}. \quad [4]$$

Comparing [1] and [4] shows that the acceleration term is missing in [4]. The inconsistency in pressure drop calculations by using the two equivalent methods results from the erroneous assumption of a cylindrical Taylor bubble with a constant void along the bubble. A curved nose of the gas bubble (figure 2) is essential for a consistent calculation of the pressure drop in slug flow, independent of the method used. It will be shown later that the acceleration term in the mixing zone of the liquid slug is equal to the sum of gravitational and shear losses in the liquid film adjacent to the curved nose of the Taylor bubble (figure 2), before the falling film reaches its terminal thickness.

HYDRODYNAMIC PARAMETERS AND PRESSURE DROP CALCULATIONS FOR A TAYLOR BUBBLE WITH A CURVED NOSE

A schematic diagram of the slug flow is presented in figure 2. Large Taylor bubbles of length l_{TB}, move steadily upward with a translational velocity U_T. These bubbles are long cylindrical voids having a curved nose and a flat tail. The Taylor bubbles are followed by liquid slugs containing small bubbles that are distributed almost uniformly over the pipe cross-section and over the length of the liquid slug, with a bulk void concentration, ϵ_s ($= 1 - R_s$). The liquid film is decelerated along

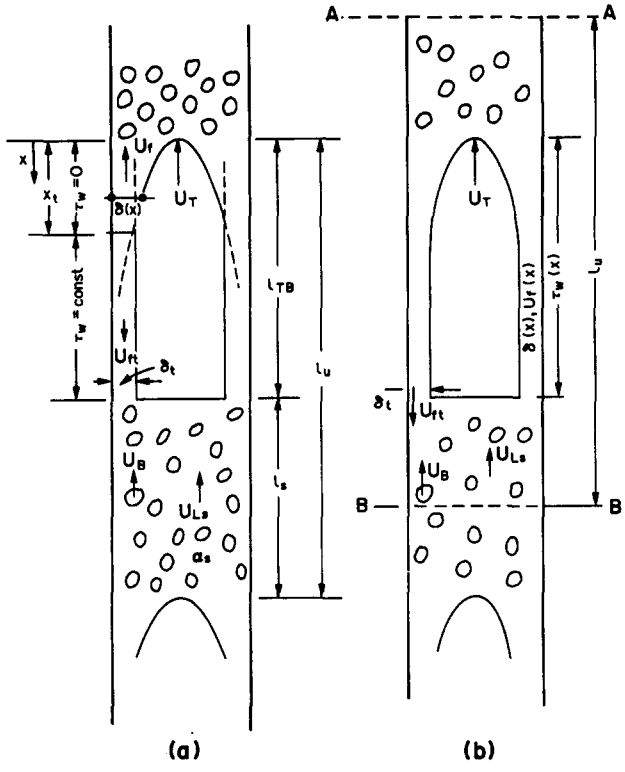

Figure 2. Slug flow structure.

the Taylor bubble until it reaches a zero velocity and changes direction to a falling film. The film thickness is continually narrowed until it is stabilized under the action of the friction force at the wall (if the bubble is long enough). In this case the film attains its terminal film thickness δ_t, and the corresponding terminal velocity, U_{ft}. This description of the Taylor bubble profile and film velocity in vertical slug flow has been experimentally verified by Nakoryakov *et al.* (1986) who measured the value and direction of the instantaneous wall shear stress and the liquid velocity along a slug unit.

The slug unit length (l_u) and the liquid holdup and velocity of the film at the bottom of the bubble will now be predicted on the basis of the above-described structure (figure 2). The effect of assuming a flat nose instead of a curved nose on the pressure drop calculations will be shown.

Slug Flow Parameters

The total volumetric flow rate, $U_M A$, is constant across any cross-section, therefore:

$$U_M = U_{LS} + U_{GS} = U_{Ls}(1 - \epsilon_s) + U_B \epsilon_s \qquad [5]$$

where U_M is the total mixture velocity, U_{LS} and U_{GS} are the liquid and gas superficial velocities, U_{Ls} is the velocity of the liquid in the liquid slug, U_B is the velocity of the gas bubbles in the liquid slug and ϵ_s the void fraction of the liquid slug.

The translational velocity of a Taylor bubble is assumed to be (Nicklin *et al.* 1962)

$$U_T = 1.2U_M + 0.35\sqrt{gD}, \qquad [6]$$

where D is the pipe diameter.

The body of the liquid slug is assumed to behave as a fully developed bubble flow. The average axial velocity of the bubbles, U_B, may be expressed by

$$U_B = U_M + U_0, \qquad [7]$$

where U_0, the bubble rise velocity due to buoyancy, is calculated by (Harmathy 1960)

$$U_0 = 1.53\left[\frac{g(\rho_L - \rho_G)\sigma}{\rho_L^2}\right]^{1/4}. \quad [8]$$

Using [5] and [7],

$$U_{Ls} = U_M - \frac{U_0 \epsilon_s}{1 - \epsilon_s}. \quad [9]$$

For large-diameter pipes, the gas velocity in the Taylor bubbles U_G exceeds that of the dispersed bubble, U_B (Taitel *et al.* 1980), in addition the liquid film seems to be essentially free of small bubbles. The physical picture that is consistent with the above description is that the dispersed bubbles in the liquid slug coalesce at the nose of the Taylor bubble, while gas bubbles are re-entrained from the back of the Taylor bubble into the liquid slug.

A liquid mass balance over a slug unit results in

$$AU_{LS} = \frac{1}{\tau}\int_0^{\tau}(U_L A_L)\,dt = \frac{1}{\tau}\left(U_{Ls}A_{Ls}t_s + \int_0^{t_f} A_f U_f\,dt\right)$$

or

$$U_{LS} = U_{Ls}(1 - \epsilon_s)\frac{l_s}{l_u} + \int_0^{l_{TB}} R_f U_f \frac{dx}{l_u}, \quad [10]$$

where τ is the time for passage of a slug unit, l_s is the length of the liquid slug, l_{TB} the length of the Taylor bubble and l_u the length of a slug unit, R_f is the local holdup of the liquid film ($=A_f/A$), U_f is the corresponding average film velocity (positive for upward flow) and x is an axial coordinate along the film (figure 2).

A liquid mass balance relative to a coordinate system that moves with a translational velocity, U_T, yields

$$R_f(U_T - U_f) = R_s(U_T - U_{Ls}), \quad [11]$$

where R_s is the average liquid holdup within the liquid slug ($=1-\epsilon_s$).

Inserting [11] and [5] into [10] results in

$$U_{GS} = U_B\epsilon_s + U_T R_s\frac{l_{TB}}{l_u} - U_T\int_0^{l_{TB}} R_f\frac{dx}{l_u}. \quad [12]$$

As has been mentioned before, for sufficiently long bubbles, gravity in the film is balanced by wall shear forces and the film thickness attains a terminal constant value, δ_t, which is given by (Wallis 1969)

$$\frac{\delta_t}{D} = k\left[\frac{\mu_L^2}{D^3 g(\rho_L - \rho_G)\rho_L}\right]^{1/3}\left(\frac{4\Gamma}{\mu_L}\right)^m, \quad [13]$$

where Γ is the mass flow rate per unit peripheral length, ($\Gamma = \rho_L|U_{ft}|\,\delta_t$), U_{ft} is the terminal velocity of the developed falling film. For laminar flow, k and m equal 0.909 and 1.3, respectively. For turbulent film flow ($\mathrm{Re}_f = 4\Gamma/\mu_L > 1000$), Wallis suggested $k = 0.115$ and $m = 0.6$. Fernandes *et al.* (1983) strongly recommend the relation proposed by Brotz (1954) which suggests $k = 0.0682$ and $m = 2/3$, these are the values used in this work.

The liquid holdup in the film R_f is directly related to the film thickness, δ, by

$$R_f = 4\frac{\delta}{D} - 4\left(\frac{\delta}{D}\right)^2. \quad [14]$$

Equation [13] together with [14], [11] and [9], can now be solved to yield the solution for the terminal film velocity U_{ft} and the terminal film thickness, δ_t or the film holdup R_{ft}.

Two cases are considered. The first case is an approximate one in which viscous forces along the curved nose of the Taylor bubble are negligible [figure 2(a)]. This allows an analytical solution for the bubble shape, its length and the film velocity and thickness at the bottom of the bubble

(U_{fe}, δ_{fe}). In the second case, a wall shear stress is considered also in the curved region of the Taylor bubble [figure 2(b)].

Case 1

The Taylor bubble in this case is assumed to consist of a nose region in which the liquid is accelerated under gravity, and a lower region in which gravity is balanced by wall shear stress and the film thickness is constant. The relative velocity of the liquid film in the nose region is accelerated from $U_{r0} = U_T - U_{Ls}$ at the bubble's top to $U_{rx} = U_T - U_f$ at a distance x from the bubble top.

Momentum and mass balances on the liquid film, relative to a coordinate system moving with a velocity U_T, yields

$$U_{rx}^2 = U_{r0}^2 = 2g\left(1 - \frac{\rho_G}{\rho_L}\right)x, \qquad [15]$$

$$U_{rx} R_f = U_{r0} R_s. \qquad [16]$$

Solving [15] and [16] for R_f yields

$$R_f(x) = \frac{R_s}{\sqrt{\dfrac{2g\rho' x}{(U_T - U_{Ls})^2} + 1}}, \qquad [17]$$

where $\rho' = 1 - \rho_G/\rho_L$.

This relation is applicable until the film reaches its terminal thickness (R_{ft}) (as predicted by [13]) at a distance x_t [figure 2(a)] from the bubble top.

The length of the Taylor bubble, l_{TB}, is now found by using the mass balance [12]. For Taylor bubbles shorter than x_t [figure 2(a)], the following equation is obtained:

$$U_{GS} = U_B(1 - R_s) + U_T R_s \frac{l_{TB}}{l_s + l_{TB}} - U_T R_s \frac{(U_T - U_{Ls})^2}{g\rho'(l_s + l_{TB})}\left[\sqrt{1 + \frac{2g\rho' l_{TB}}{(U_T - U_{Ls})^2}} - 1\right]; \qquad [18]$$

while for Taylor bubbles longer than x_t the mass balance yields

$$U_{GS} = U_B(1 - R_s) + U_T R_s \frac{l_{TB}}{l_s + l_{TB}} - U_T R_s \frac{(U_T - U_{Ls})^2}{g\rho'(l_s + l_{TB})}\left[\sqrt{1 + \frac{2g\rho' x_t}{(U_T - U_{Ls})^2}} - 1\right] - \frac{U_T}{l_s + l_{TB}} R_{ft}(l_{TB} - x_t). \qquad [19]$$

The solution of [18] and [19] requires information regarding R_s and l_s. These parameters were estimated using the method suggested by Barnea & Brauner (1985).

Note that for the special case of a cylindrical Taylor bubble with a flat nose, [19] is reduced to the following commonly used equation:

$$\frac{l_{TB}}{l_{TB} + l_s} = \frac{U_{LS} - U_{Ls} R_s}{R_{ft} U_{ft} - U_{Ls} R_s} = \frac{U_{GS} - U_B \epsilon_s}{U_T R_s - U_T R_{ft}}. \qquad [20]$$

Case 2

A more exact approach is to consider frictional losses also along the curved region of the Taylor bubble (that were previously neglected).

The momentum equation [figure 2(b)] on the liquid film for this case is

$$\frac{\tau_w S_w}{A} + (\rho_L - \rho_G) R_f g = \rho_L R_f (U_T - U_f) \frac{d(U_T - U_f)}{dx}, \qquad [21]$$

where

$$\frac{\tau_w S_w}{A} = \tfrac{1}{2} f_w \rho_L U_f |U_f| \frac{4}{D}. \qquad [22]$$

The value of f_w was obtained from the Wallis correlation for the terminal film thickness, [13]. For turbulent film flow $f_w = 0.01015$, while for laminar flow $f_w = 24/\mathrm{Re}_f$.

Using the mass balance [11] results in the following differential equation for U_f:

$$\frac{dU_f}{dx} = -\left\{\left[\frac{g\rho'}{(U_T - U_f)} + \frac{\frac{2}{D}f_w}{(U_T - U_{Ls})R_s}\right]U_f|U_f|\right\}, \quad [23]$$

where U_f is positive for upward film flow and negative for downward flow at $x = 0$, $U_f = U_{Ls}$ and $R_f = R_s$.

The differential equation [23] is solved numerically for $U_f(x)$ and the corresponding $R_f(x)$ is found using [11]. The length of the Taylor bubble, l_{TB} as well as U_{fe} and R_{fe}, at the bottom of the Taylor bubble are found now by satisfying the mass balance of [12].

The estimation of the above-mentioned hydrodynamic parameters, which depend on the actual bubble shape, enable one to perform a consistent calculation of the pressure drop in slug flow independent of the location of the cut planes of the control volume of the slug unit (figure 2).

Pressure Drop Calculations

Since the pressure drop along the Taylor bubble is negligible the total pressure loss across one slug unit is

$$\Delta P_t = \Delta P_{acc} + \Delta P_{fs} + \Delta P_{gs}, \quad [24]$$

where ΔP_{acc} is the pressure drop associated with the acceleration of the slow moving liquid in the film to the liquid velocity within the liquid slug:

$$\Delta P_{acc} = (U_{Ls} - U_{fe})(U_T - U_{Ls})\rho_L R_s. \quad [25]$$

The pressure loss due to frictional effects in the liquid slug is

$$\Delta P_{fs} = \frac{2f_s}{D}\rho_s U_M^2 l_s, \quad [26]$$

where

$$\rho_s = \rho_L R_s + \rho_G(1 - R_s) \quad [27]$$

and f_s is the friction factor based on the mixture Reynolds number within the liquid slug.

The pressure drop due to the hydrostatic head is

$$\Delta P_{gs} = \rho_s g l_s. \quad [28]$$

An alternative way to calculate the total pressure drop is to consider a global force balance over the control volume A–A–B–B (figure 2):

$$\Delta P_t = \rho_u g l_u + \int_0^{l_u} \frac{\tau_w S_w \, dx}{A}, \quad [29]$$

where ρ_u is the average density of the slug unit,

$$\rho_u = \epsilon_u \rho_G + (1 - \epsilon_u)\rho_L. \quad [30]$$

The volume average void fraction over a slug unit ϵ_u is

$$\epsilon_u = \frac{A\epsilon_s l_s + \int_0^{l_{TB}} A_G \, dx}{A \cdot l_u}. \quad [31]$$

Substituting [12] for $\int_0^{l_{TB}} A_G \, dx$ yields the following expression for ϵ_u:

$$\epsilon_u = \frac{U_{GS} - U_B\epsilon_s + U_T\epsilon_s}{U_T}. \quad [32]$$

Equation [32] is a very interesting result by itself. It shows that the average void fraction of a slug unit depends on the liquid and gas flow rates (U_{GS}, U_{LS}), the bubble rise velocity U_0, the translational velocity U_T and the void fraction within the liquid slug ϵ_s, and it is independent of the *bubble shape*, the bubble length, the liquid slug length and the film thickness.

Thus, for the calculation of the average hydrostatic pressure drop ($\rho_u g$) one does not need to calculate the hydrodynamic parameters of the slug flow. However, in order to calculate the second term on the r.h.s. of [29] (the pressure gradient due to friction), one needs information regarding the distribution of the shear losses along a single slug unit. In order to calculate it the bubble profile $R_f(x)$ as well as the axial film velocity distribution $U_f(x)$ are needed.

Note that for the case where a cylindrical bubble with a flat nose is assumed, [24] yields pressure drops which are large by ΔP_{acc} compared to the pressure drop results obtained from [29], as has been demonstrated by [1] and [4] (which are equivalent to [24] and [29], respectively). However, when the shape of the nose is taken into account both [24] and [29] yields identical results. Referring to [21] and [11], the integrated momentum balance on the curved region of the film yields

$$\rho_L R_s (U_T - U_{Ls})(U_{Ls} - U_{fe}) = (\rho_L - \rho_G) g \int_0^{x_t} R_f \, dx + \int_0^{x_t} \frac{\tau_w S_w}{A} \, dx. \qquad [33]$$

As seen, the l.h.s. of [33] is equal to the acceleration losses in the mixing zone of the liquid slug, ΔP_{acc} [25]. Namely, ΔP_{acc} in [24] is equal to the sum of gravitational and frictional losses of the liquid film in the curved zone of the bubble. Thus, for a curved nose bubble the calculation of the pressure drop via [24] is identical to the calculation via [29] (a slight difference exists owing to the common neglect of the gas gravity within the Taylor bubble in [24]). However, for a cylindrical Taylor bubble with a flat nose the frictional losses in the liquid film are balanced by gravity and the use of [29] for the pressure drop calculation leads to [4], where the acceleration term in the mixing zone of the liquid slug is missing.

So far two methods for the evaluation of the bubble shape have been presented, cases 1 and 2. Both cases lead to a consistent pressure drop calculation using either [24] or [29]. These two "consistent" modes of pressure drop calculation will be now compared with other approximate modes for the purpose of estimating the errors incurred using a cylindrical shape.

In summary the following modes of pressure drop calculation in slug flow will be compared.

Mode 1

The bubble shape is evaluated according to case 1, where frictional losses in the bubble head zone are neglected. The pressure drop is calculated by using either [24] or [29], which yield identical results.

Mode 2

The bubble shape is evaluated according to case 2, where viscous forces are considered also in the nose zone. Pressure drop, again, is calculated by [24] or [29]. This is the most accurate method used here.

Mode 3

A cylindrical bubble with a flat nose is considered. The pressure drop is calculated by [24], where the acceleration term is used. This method has been widely used in the literature (Fernandes *et al.* 1983; Sylvester 1987).

Mode 4

A cylindrical bubble with a flat nose is considered. The pressure drop is calculated by using [29]. The use of [29] for a flat nose bubble is equivalent to the use of [24] and ignoring the term of acceleration (ΔP_{acc}). This method has been used by Orell & Rembrand (1986).

Mode 5

This is an approximate method for which no prior information regarding the slug geometry is needed. As has been shown, the average void fraction ϵ_u is independent of the bubble shape, the bubble length, the liquid slug length and the film thickness, [32]. This allows an accurate calculation

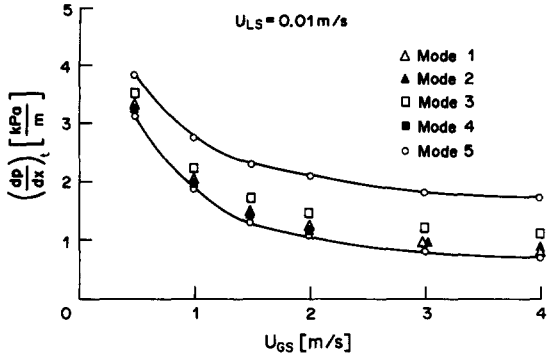

Figure 3. Pressure drop calculations for slug flow. Air–water, 0.1 MPa, 25°C, 5 cm dia, $U_{LS} = 0.01$, $l_s = 16D$.

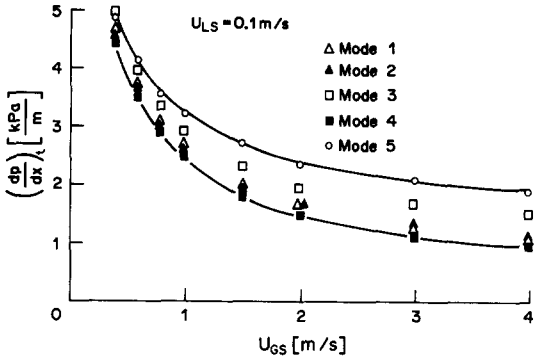

Figure 4. Pressure drop calculations for slug flow. Air–water, 0.1 MPa, 25°C, 5 cm dia, $U_{LS} = 0.1$, $l_s = 16D$.

of the gravitational pressure drop of the slug unit. However, the calculation of the frictional pressure drop requires information regarding the velocity distribution in the liquid along a slug unit. Several approximate methods for the average shear stress have been recommended in the literature (Spedding *et al.* 1982). One of the commonly used methods is to evaluate the average wall shear stress as for a single equivalent fluid moving at the average mass velocity:

$$\left(\frac{dp}{dx}\right)_{fu} = \frac{2}{D} f_M \rho_u V_M^2, \qquad [34]$$

where

$$V_M = \frac{U_{LS}\rho_L + U_{GS}\rho_G}{\rho_u} \qquad [35]$$

and f_M is the wall shear stress based on the velocity, V_M. Equation [34] is the frictional term in the drift flux model.

By inserting the frictional term suggested by [34] into [29] the pressure drop in slug flow can be calculated without the *a priori* estimation of the slug structure. This method will be compared with modes 1 and 2 and the conditions under which this simple method is applicable will be tested.

RESULTS AND DISCUSSION

Figures 3–6 present a comparison between the five modes for pressure drop calculations. The comparison was performed for an air–water system over the whole space in which slug flow occurs.

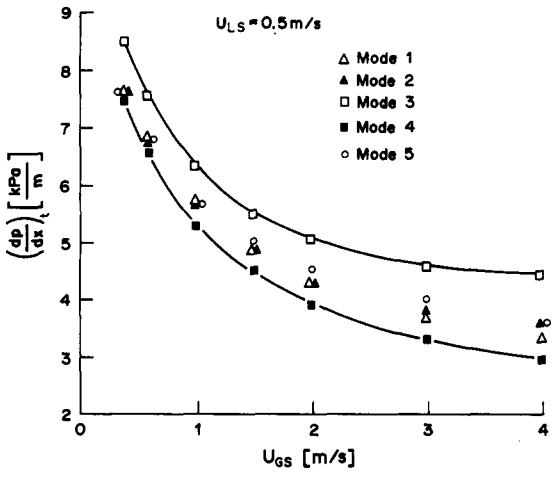

Figure 5. Pressure drop calculations for slug flow. Air–water, 0.1 MPa, 25°C, 5 cm dia, $U_{LS} = 0.5$, $l_s = 16D$.

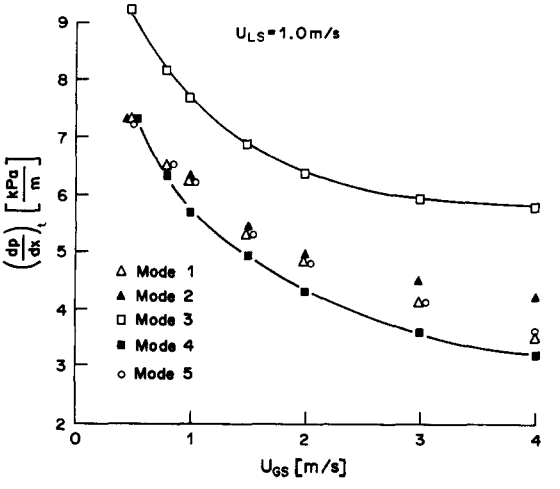

Figure 6. Pressure drop calculations for slug flow. Air–water, 0.1 MPa, 25°C, 5 cm dia, $U_{LS} = 1$, $l_s = 16D$.

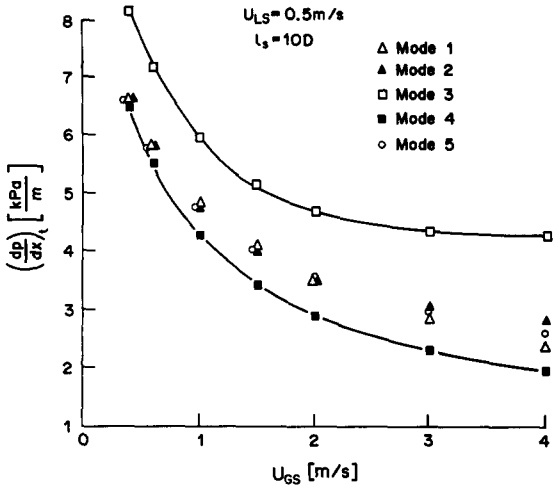

Figure 7. Pressure drop calculations for slug flow. Air–water, 0.1 MPa, 25°C, 5 cm dia, $U_{LS} = 0.5$, $l_s = 10D$.

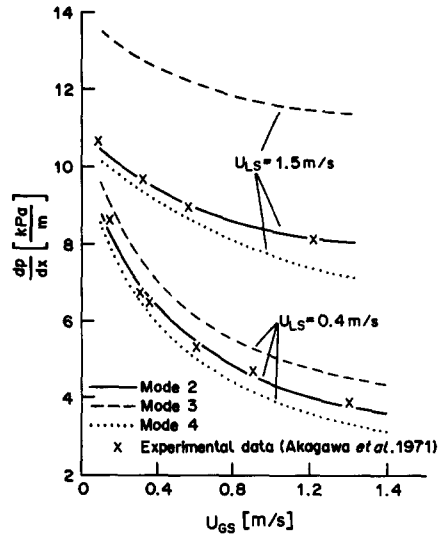

Figure 8. Comparison with experimental results. Air–water, 0.1 MPa, 25°C, 2.8 cm dia.

The values of l_s and R_s used here were evaluated by the method presented by Barnea & Brauner (1985). l_s was taken as $16D$ and the value of R_s was calculated by

$$R_s = 1 - 0.058\left\{2\left[\frac{0.4\sigma}{(\rho_L - \rho_G)g}\right]^{1/2}\left(\frac{2f_s}{D}U_M^3\right)^{2/5}\left(\frac{\rho_L}{\sigma}\right)^{3/5} - 0.725\right\}^2. \quad [36]$$

Note that for large-diameter pipes ($D > 0.05$ m for air–water) the maximum value of R_s is 0.75 (Barnea & Brauner 1985).

As has been demonstrated, the "right" way of calculation is via mode 1 or 2. The two methods lead to almost the same results. This justifies the assumption that near the nose viscous forces are negligible. Note also that the liquid velocity in the nose zone changes direction, resulting in a negligible net contribution of the wall shear stress to the pressure drop.

Mode 3, in which a cylindrical Taylor bubble is considered and the acceleration pressure drop is taken into account, overpredicts the results obtained by modes 1 and 2. The discrepancy is relatively small at low liquid and gas flow rates. At high liquid flow rates the discrepancy is more pronounced along the whole range of gas flow rates. These higher values stem from two reasons: (1) the calculated value of the slug unit, l_u is slightly shorter for a bubble with a flat nose; and (2) the film velocity at the bottom of a flat nose bubble is always U_{ft}, which is the maximum negative velocity of the liquid film—this increases the contribution of the acceleration term in [24] relative to that obtained for a curved nose bubble. For high liquid flow rates this tendency is more pronounced.

Estimating a bubble with a flat nose, while ignoring the term of acceleration in [24], mode 4, underpredicts the pressure drop results compared to modes 1 and 2. However, the discrepancy now is lower, especially at high liquid flow rates.

Mode 5 overpredicts the pressure drop calculation considerably at low liquid rates (figures 3 and 4) while at high liquid flow rates the results are almost identical to those of modes 1 and 2 (figures 5 and 6). The reason is that at high liquid flow rates the liquid holdup is high and the overall gravitational term $\rho_u g$ in [29] is dominant, thus the accurate evaluation of τ_w is not essential. While at low liquid flow rates the negative wall shear stress along the falling film that oppose the direction of gravity becomes significant.

The sensitivity of the pressure drop to the liquid slug length is examined in figure 7. As would be expected, modes 4 and 5 are independent of the value of l_s and modes 1 and 2 are insensitive to the choice of l_s in the range $l_s = 10D$ to $30D$ (which is the observed experimental range for l_s). On the other hand, mode 3, which assumes a flat nose and considers the acceleration term is sensitive to the choice of l_s. A short l_s increases the contribution of the acceleration pressure drop considerably and increases the error of this model.

Although the main objective of this work is to point out the theoretical inconsistency of the former methods that have been used for pressure drop calculations, it should be mentioned that the suggested method compares very well with experimental results over a wide range of liquid and gas flow rates (Akagawa *et al.* 1971). Figure 8 demonstrates this agreements for two liquid flow rates. As can be seen, mode 2 is very close to the experimental results, mode 3, which considers a bubble with a flat nose with acceleration, overpredicts the experimental results, especially for high liquid flow rates, while, mode 4, which uses a uniform film thickness but ignores acceleration, slightly underpredicts the experimental data.

SUMMARY AND CONCLUSIONS

1. The assumption of a cylindrical Taylor bubble with a flat nose may yield erroneous results for pressure drop calculations in vertical slug flow.
2. A curved shape of the Taylor bubble's nose is essential for consistent calculations of the pressure drop, independent of the choice of the control volume that is used for this calculation (a global one or the liquid slug only).
3. The approximate method which considers a bubble with a flat nose and incorporates the acceleration term (mode 3) always overpredicts the results obtained by modes 1 and 2, where a curved shape is assumed. The discrepancy is more pronounced at high liquid flow rates. At low liquid flow rates this approximation is reasonable.
4. The approximate method which considers a bubble with a flat nose but ignores the acceleration term (mode 4) usually yields lower pressure drop results than those obtained by modes 1 and 2. This method, however, is preferred to the method where the acceleration pressure drop term is used.
5. The approximate method presented by mode 5, where no prior information regarding the slug geometry is needed, yields good results at relatively high liquid flow rates, whereas for low liquid flow rates this method yields pressure drop results that are higher than those predicted by the accurate methods (modes 1 and 2).
6. The average liquid holdup is independent of the bubble shape, the bubble length and the liquid slug length, [32]. Thus, for the calculation of the hydrostatic pressure drop one does not need information regarding the slug structure.
7. Finally, it should be stressed that the main purpose of this work is to clarify the inconsistency caused by the neglect of the nose curvature and the use of the acceleration term rather than to provide the quantitative numerical inaccuracies incorporated in the approximate calculations.

REFERENCES

AKAGAWA, K., HAMAGUCHI, H., SAKAGUCHI, T. & IKARI, T. 1971 Studies on the fluctuation of pressure drop in two-phase slug flow. *Bull. JSME* **14,** 447–454.

BARNEA, D. & BRAUNER, N. 1985 Hold-up of the liquid slug in two phase intermittent flow. *Int. J. Multiphase Flow* **11,** 43–49.

BROTZ, W. 1954 Uber die vorausberechnung der absorptionsgeschwindigkeit von gasen in stromenden flussigkeitsschichten. *Chemie-Ingr-Tech.* **26,** 470.

FERNANDES, R. C., SEMIAT, R. & DUKLER, A. E. 1983 Hydrodynamic model for gas–liquid slug flow in vertical tubes. *AIChE Jl* **29,** 981–989.

HARMATHY, T. Z. 1960 Velocity of large drops and bubbles in media of infinite or restricted extent. *AIChE Jl* **6,** 281–288.

NAKORYAKOV, V. E., KASHINSKY, O. N. & KOZMENKO, B. K. 1986 Experimental study of gas–liquid slug flow in a small-diameter vertical pipe. *Int. J. Multiphase Flow* **12,** 337–355.

NICKLIN, D. J., WILKES, J. O. & DAVIDSON, J. F. 1962 Two-phase flow in vertical tubes. *Trans. Instn chem. Engrs* **40,** 61–68.

ORELL, A. & REMBRAND, R. 1986 A model for gas–liquid slug flow in a vertical tube. *Ind. Engng Chem. Fundam.* **25,** 196–206.

SPEDDING, P. L., CHEN, J. J. J. & VAN NGUYEN, T. 1982 Pressure drop in two phase gas–liquid flow in inclined pipes. *Int. J. Multiphase Flow* **8,** 407–431.

SYLVESTER, N. D. 1987 A mechanistic model for two phase vertical slug flow in pipes. *J. Energy Res. Technol.* **109,** 206–213.

TAITEL, Y. & BARNEA, D. 1983 Counter current gas liquid vertical flow—model for flow pattern and pressure drop. *Int. J. Multiphase Flow* **9,** 637–647.

TAITEL, Y., BARNEA, D. & DUKLER, A. E. 1980 Modelling flow pattern transitions for steady upward gas–liquid flow in vertical tubes. *AIChE Jl* **26,** 345–354.

WALLIS, G. B. 1969 *One-dimensional Two-phase Flow*. McGraw-Hill, New York.